FULL PAPER

Dalton
www.rsc.org/dalton

Structure and dioxygen-reactivity of copper(I) complexes supported by bis(6-methylpyridin-2-ylmethyl)amine tridentate ligands†‡

Takao Osako,[a] Shohei Terada,[b] Takehiko Tosha,[c] Shigenori Nagatomo,[c] Hideki Furutachi,[b] Shuhei Fujinami,[b] Teizo Kitagawa,[c] Masatatsu Suzuki[b] and Shinobu Itoh*[a]

[a] *Department of Chemistry, Graduate School of Science, Osaka City University, 3-3-138 Sugimoto, Sumiyoshi-ku, Osaka, 558-8585, Japan. E-mail: shinobu@sci.osaka-cu.ac.jp*

[b] *Department of Chemistry, Faculty of Science, Kanazawa University, Kakuma-machi, Kanazawa, Ishikawa, 920-1192, Japan*

[c] *Okazaki Institute for Integrative Bioscience, National Institutes of Natural Sciences, Myodaiji, Okazaki, 444-8787, Japan*

Received 6th January 2005, Accepted 15th March 2005
First published as an Advance Article on the web 23rd September 2005

The structure and dioxygen-reactivity of copper(I) complexes $\mathbf{2}^{R}$ supported by *N*,*N*-bis(6-methylpyridin-2-ylmethyl)-amine tridentate ligands L2^{R} [R (*N*-alkyl substituent) = $-CH_2Ph$ (Bn), $-CH_2CH_2Ph$ (Phe) and $-CH_2CHPh_2$ (PhePh)] have been examined and compared with those of copper(I) complex $\mathbf{1}^{Phe}$ of *N*,*N*-bis[2-(pyridin-2-yl)ethyl]amine tridentate ligand L1^{Phe} and copper(I) complex $\mathbf{3}^{Phe}$ of *N*,*N*-bis(pyridin-2-ylmethyl)amine tridentate ligand L3^{Phe}. Copper(I) complexes $\mathbf{2}^{Phe}$ and $\mathbf{2}^{PhePh}$ exhibited a distorted trigonal pyramidal structure involving a d–π interaction with an η^1-binding mode between the metal ion and one of the *ortho*-carbon atoms of the phenyl group of the *N*-alkyl substituent [$-CH_2CH_2Ph$ (Phe) and $-CH_2CHPh_2$ (PhePh)]. The strength of the d–π interaction in $\mathbf{2}^{Phe}$ and $\mathbf{2}^{PhePh}$ was weaker than that of the d–π interaction with an η^2-binding mode in $\mathbf{1}^{Phe}$ but stronger than that of the η^1 d–π interaction in $\mathbf{3}^{Phe}$. Existence of a weak d–π interaction in $\mathbf{2}^{Bn}$ in solution was also explored, but its binding mode was not clear. Redox potentials of the copper(I) complexes ($E_{1/2}$) were also affected by the supporting ligand; the order of $E_{1/2}$ was $\mathbf{1}^{Phe} > \mathbf{2}^{R} > \mathbf{3}^{Phe}$. Thus, the order of electron-donor ability of the ligand is L1^{Phe} < L2^{R} < L3^{Phe}. This was reflected in the copper(I)–dioxygen reactivity, where the reaction rate of copper(I) complex toward O_2 dramatically increased in the order of $\mathbf{1}^{R} < \mathbf{2}^{R} < \mathbf{3}^{R}$. The structure of the resulting Cu_2/O_2 intermediate was also altered by the supporting ligand. Namely, oxygenation of copper(I) complex $\mathbf{2}^{R}$ at a low temperature gave a (μ-η^2:η^2-peroxo)dicopper(II) complex as in the case of $\mathbf{1}^{Phe}$, but its O–O bond was relatively weakened as compared to the peroxo complex derived from $\mathbf{1}^{Phe}$, and a small amount of a bis(μ-oxo)dicopper(III) complex co-existed. These results can be attributed to the higher electron-donor ability of L2^{R} as compared to that of L1^{Phe}. On the other hand, the fact that $\mathbf{3}^{Phe}$ mainly afforded a bis(μ-oxo)dicopper(III) complex suggests that the electron-donor ability of L2^{R} is not high enough to support the higher oxidation state of copper(III) of the bis(μ-oxo) complex.

Introduction

Bis(pyridin-2-ylalkyl)amine tridentate ligands have been playing very important roles in copper/dioxygen (Cu/O_2) chemistry.[1–5] It has been well established that copper(I) complexes of bis[2-(pyridin-2-yl)ethyl]amine tridentate ligands (L1^{R}, Chart 1) predominantly afford (μ-η^2:η^2-peroxo)dicopper(II) complexes **A** (Chart 2) in the reaction with O_2 at a low temperature.[1–4] The peroxo complexes **A** supported by L1^{R}-type ligands have been extensively studied as structural and functional models of oxy-hemocyanin and oxy-tyrosinase on their ability of reversible dioxygen binding and aromatic hydroxylation reaction.[6–10] Recently, Itoh and co-workers have also demonstrated that adoption of the bis(pyridin-2-ylmethyl)amine tridentate ligand L3^{R} [R = $-CH_2CH_2Ph$ (Phe), Chart 1] instead of L1^{R} induces O–O bond cleavage of the peroxo complex **A** to give a bis(μ-oxo)dicopper(III) complex **B** in the reaction of the copper(I) complex and O_2 under similar reaction conditions.[11] The shorter alkyl linker chain (methylene) in L3^{R} affords a smaller five-membered chelate ring with increasing electron donor ability

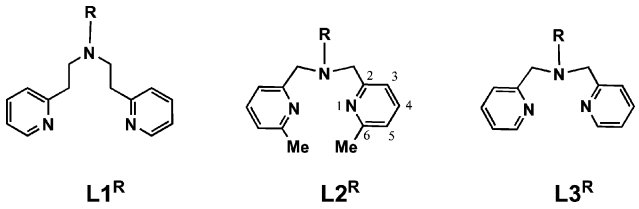

Chart 1

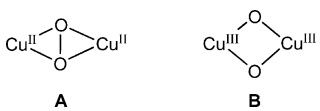

Chart 2

of pyridine,[12] thus enhancing the O–O bond cleavage and stabilizing the higher oxidation state of copper(III) in **B**. The electron-donor ability of pyridine can be also tuned by the C-4 substituents on the pyridine nucleus of L1^{R}-type ligand, affecting the equilibrium position between **A** and **B** in solution, where the electron-donating substituent such as NMe_2 weakens the O–O bond and increases the ratio of **B** in the equilibrium.[13]

In the case of TPA tetradentate ligand system (TPA = tris(pyridin-2-ylmethyl)amine), on the other hand, the presence of a methyl substituent at the 6-position of pyridine nucleus has been well demonstrated to induce large effects not

† Based on the presentation given at Dalton Discussion No. 8, 7–9th September 2005, University of Nottingham, UK.

‡ Electronic supplementary information (ESI) available: Spectral change for the titration of $\mathbf{2}^{Phe}$ by CH_3CN (Fig. S1) and Arrhenius plots for the oxygenation reaction of $\mathbf{2}^{Phe}$ and $\mathbf{2}^{PhePh}$ (Fig. S2). See DOI: 10.1039/b500202h

DOI:10.1039/b500202h

only on Cu/O_2 chemistry but also on iron/dioxygen (Fe/O_2) chemistry.[2,14–16] The 6-methyl group has been shown to cause a decrease of electron-donor ability of pyridine due to steric repulsion between the substituent and the bound metal ion.[17] We have recently found a similar effect of 6-methylpyridine in the $L1^R$-type tridentate ligand system, where the reactivity of copper(I) complex $[Cu^I(L1^{Phe})(MeCN)]^+$ (Phe = $–CH_2CH_2Ph$) toward O_2 is significantly diminished when a methyl group is introduced into the 6-position of the pyridine nucleus of $L1^{Phe}$.[18] In this case, the weaker donor ability of the 6-methylpyridine induces stronger binding of MeCN to copper(I), thus prohibiting the reaction of copper(I) toward O_2.

As our continuing efforts to understand the factors that control the copper(I)–dioxygen reactivity in the pyridylalkylamine tridentate ligand system, we herein investigated the structure and reactivity of the copper(I) complexes of $L2^R$, bis(6-methylpyridin-2-ylmethyl)amine tridentate ligands [R = $–CH_2Ph$ (Bn), $–CH_2CH_2Ph$ (Phe) and $–CH_2CHPh_2$ (PhePh), Chart 1]. The results demonstrated that not only the structure of the copper(I) complex but also strength of the O–O bond of side-on peroxo complex is significantly affected by the 6-methyl substituent.

Experimental

General

All chemicals used in this study except the ligands and the complexes were commercial products of the highest available purity and were further purified by the standard methods, if necessary.[19] FT-IR spectra were recorded with a Shimadzu FTIR-8200PC or a Horiba FT-200 spectrophotometer. UV-vis spectra were measured using a Hewlett Packard HP8453 diode array spectrophotometer equipped with a Unisoku thermostated cell holder designed for low-temperature measurements (USP-203) or a Shimadzu diode array spectrometer Multispec-1500 equipped with the same cell holder. Mass spectra were recorded with a JEOL JMS–700T Tandem MS station or a PE SCIEX API 150EX (for ESI-MS). ESI-TOF/MS spectra were measured with a Micromass LCT spectrometer. NMR spectra were recorded on a Bruker Avance 600 spectrometer or a JEOL JNM-LM400. ^1H NMR spectra were referenced to the residual proton resonance of the solvent and ^{13}C NMR spectra to the solvent resonance (CD_2Cl_2: ^1H, δ 5.32, ^{13}C, δ 53.8). Complete peak assignments in the ^1H and ^{13}C NMR spectra of ligands $L2^{Phe}$ and $L2^{PhePh}$ and their copper(I) complexes have been accomplished by employing 2D NMR techniques (COSY, NOESY, HMQC and HMBC).

Electrochemical measurements

The cyclic voltammetry (CV) measurements were performed on an ALS–630A electrochemical analyzer in anhydrous CH_2Cl_2 containing 0.1 M NBu_4ClO_4 as a supporting electrolyte. The Pt working electrode was polished with a polishing alumina suspension and rinsed with CH_2Cl_2 before use. The counter-electrode was a Pt wire. A silver pseudo-reference electrode was used, and the potentials were determined using the ferrocene–ferrocenium (Fc/Fc^+) couple as a reference. All electrochemical measurements were carried out at 25 °C under an atmospheric pressure of Ar in a glove box (Miwa Co. Ltd.).

Visible resonance Raman measurements

The 514.5 nm line of an Ar^+ laser (Model GLG3200, NEC) was used as the exciting source. Visible resonance Raman scattering was detected with a liquid nitrogen cooled CCD detector (Model LN/CCD-1340 × 400PB, Princeton Instruments) attached to a 1 m single polychromator (Model MC-100DG, Ritsu Oyo Kogaku). The slit width and slit height were set to be 150 μm and 20 mm, respectively. The spectral slit width is 5.7 cm^{-1}. The wavenumber per single channel is 0.69 cm^{-1}. The laser power used was 10 mW at the sample point. All measurements were carried out with a spinning cell (1000 rpm) at −80 to −100 °C. Raman shifts were calibrated with indene and acetone, and the accuracy of the peak positions of the Raman lines was ±1 cm^{-1}.

X-Ray structure determination

Single crystals of copper(I) complexes $\mathbf{2}^{Phe}$ and $\mathbf{2}^{PhePh}$ for X-ray structural analysis were obtained by vapor diffusion of ether into a CH_2Cl_2 solution of the complex. The single crystal was mounted on a CryoLoop (Hamptom Research Co.). Data of X-ray diffraction were collected by a Rigaku RAXIS-RAPID imaging plate two-dimensional area detector using graphite-monochromated Mo-Kα radiation (λ = 0.71070 Å) to $2\theta_{max}$ of 55.0°. All the crystallographic calculations were performed by using Crystal Structure software package of the Rigaku Corporation and Molecular Structure Corporation [Crystal Structure: Crystal Structure Analysis Package version 2.0, Rigaku Corp. and Molecular Structure Corp. (2001)]. The crystal structures were solved by direct methods and refined by full-matrix least squares using SIR-92 or SHELX-97. All non-hydrogen atoms and hydrogen atoms were refined anisotropically and isotropically, respectively.

Data collection of copper(I) complexes $\mathbf{2}^{Bn}$·MeCN and $\mathbf{2}^{Bn}$·CO were carried out on a Rigaku *R*-axis IV imaging plate area detector with graphite-monochromated Mo-Kα radiation (λ = 0.71070 Å). A single crystal was mounted on the tip of a glass rod. The structures were solved by direct method (SHELX-86 for $\mathbf{2}^{Bn}$·MeCN and SIR92 for $\mathbf{2}^{Bn}$·CO) and expanded using a Fourier technique. The structures were refined by a full-matrix least-squares method by using the teXsan crystallographic software package (Molecular Structure Corporation). Non-hydrogen atoms were refined with anisotropic displacement parameters. Hydrogen atoms were positioned at calculated positions (0.95 Å). They were included, but not refined, in the final least-squares cycles.

A summary of the fundamental crystal data and experimental parameters for all the structure determinations are given in Table 1 and 2.

CCDC reference numbers 259907–259910.

See http://www.rsc.org/suppdata/dt/b5/b500202h/ for crystallographic data in CIF or other electronic format.

Kinetic measurements

Reaction of the copper(I) complex and O_2 was carried out in a 1 cm path length UV-vis cell that was held in a Unisoku thermostated cell holder USP-203 (a desired temperature can be fixed within ±0.5 °C). After the deaerated solution of the copper(I) complex (2.0×10^{-4} M) in the cell was kept at a desired temperature for several minutes, dry dioxygen gas was continuously supplied by gentle bubbling from a thin needle. Formation of the dicopper–dioxygen complex was monitored by following an increase in the absorption at 355 nm. The reaction obeyed second-order kinetics and the second-order rate constants (k_{obs}) were obtained as the slopes of linear lines of the second-order plots, $(A - A_0)/\{(A_\infty - A)[Cu]_0\}$ *vs.* time, where A_0 and A_∞ are the initial and final absorption at 355 nm and $[Cu]_0$ is the initial concentration of the copper(I) complex.

Syntheses

***N*,*N*-Bis(6-methylpyridin-2-ylmethyl)-2-phenylethylamine ($L2^{Phe}$).** Acetic acid (1.20 g, 20 mmol) was added to a methanol solution (200 mL) containing 2-phenylethylamine (1.21 g, 10 mmol) and 6-methyl-2-pyridinecarbaldehyde (2.42 g, 20 mmol), and the solution was stirred for 1 h at room temperature. $NaBH_3CN$ (1.26 g, 20 mmol) was then added slowly to the solution, and the mixture was stirred for three days at room temperature. The reaction was quenched (pH = 1) by

Table 1 Summary of the X-ray crystallographic data for complexes $\mathbf{2}^{Phe}$, $\mathbf{2}^{PhePh}$, $\mathbf{2}^{Bn}\cdot CH_3CN$ and $\mathbf{2}^{Bn}\cdot CO$

	$\mathbf{2}^{Phe}$	$\mathbf{2}^{PhePh}$	$\mathbf{2}^{Bn}\cdot CH_3CN$	$\mathbf{2}^{Bn}\cdot CO$
Empirical formula	$C_{22}H_{25}N_3CuClO_4$	$C_{28}H_{29}N_3CuClO_4$	$C_{23}H_{26}N_4CuPF_6$	$C_{22}H_{23}N_3O_5CuCl$
Formula weight	494.46	570.55	567.00	508.43
Crystal system	Monoclinic	Triclinic	Monoclinic	Triclinic
Space group (no.)	$P2_1/n$ (14)	$P\bar{1}$ (1)	$P2_1/c$ (14)	$P\bar{1}$ (2)
a/Å	11.7088(3)	7.715(4)	14.380(2)	11.159(2)
b/Å	14.6661(5)	8.887(6)	7.196(2)	17.147(2)
c/Å	12.4843(4)	9.361(6)	25.291(4)	12.387(2)
α/°		83.77(3)		88.88(1)
β/°	93.147(1)	88.29(2)	99.58(1)	109.24(1)
γ/°		75.93(3)		91.35(1)
V/Å^3	2140.6(1)	618.9(6)	2580.6(9)	2237.0(6)
Z	4	1	4	4
$F(000)$	1024.00	296.00	1160.00	1048.00
D_c/g cm^{-3}	1.534	1.531	1.459	1.510
T/°C	−115	−115	22	−120
Crystal size/mm	0.20 × 0.20 × 0.10	0.40 × 0.10 × 0.10	0.30 × 0.25 × 0.15	0.40 × 0.25 × 0.25
μ(Mo-Kα)/cm^{-1}	11.80	10.32	9.70	11.35
Diffractometer	Rigaku RAXIS-RAPID	Rigaku RAXIS-RAPID	Rigaku *R*-axis IV	Rigaku *R*-axis IV
Radiation (λ/Å)	Mo-Kα (0.71069)	Mo-Kα (0.71075)	Mo-Kα (0.71070)	Mo-Kα (0.71070)
$2\theta_{max}$/°	54.9	55.0	51.4	51.6
No. reflns. measd.	20832	5544	4365	7193
No. reflns. obsd.	3791 [$I > 3.0\sigma(I)$]	2636 [$I > 0.1\sigma(I)$]	3616 [$I > 3.0\sigma(I)$]	6582 [$I > 3.0\sigma(I)$]
No. variables	305	364	317	577
$R^{a,c}$	0.044	0.058	0.087	0.044
$R_w{}^{b,d}$	0.072	0.063	0.132	0.073
GOF	1.48	1.098	1.91	1.39

[a] $R = \sum[|F_o| - |F_c|]/\sum|F_o|$ ($I \geq 3.0\sigma(I)$ for $\mathbf{2}^{Phe}$ and $I \geq 0.1\sigma(I)$ for $\mathbf{2}^{PhePh}$). [b] $R_w = \{\sum w(|F_o| - |F_c|)^2/\sum wF_o{}^2\}^{1/2}$; $w = 1/[0.001|F_o|^2 + 3.0\sigma|F_o|^2 + 0.10]$ for $\mathbf{2}^{Phe}$ and $\mathbf{2}^{PhePh}$. [c] $R = \sum[|F_o| - |F_c|]/\sum|F_o|$ ($I \geq 2.0\sigma(I)$ for $\mathbf{2}^{Bn}\cdot$MeCN and $I \geq 3.0\sigma(I)$ for $\mathbf{2}^{Bn}\cdot$CO). [d] $R_w = [\sum w(|F_o| - |F_c|)^2/\sum w|F_o|^2]^{1/2}$; $w = 1/[\sigma^2(F_o) + p^2|F_o|^2/4]$ ($p = 0.081$ for $\mathbf{2}^{Bn}\cdot$MeCN and $p = 0.098$ for $\mathbf{2}^{Bn}\cdot$CO).

adding conc. HCl and the solvent was removed by evaporation. To the resulting material was added 15% NaOH aqueous solution (100 mL), and the organic materials were extracted with $CHCl_3$ (50 mL × 3). After drying over anhydrous K_2CO_3, evaporation of the solvent gave a brown residue, from which ligand $L2^{Phe}$ was isolated as a yellow oily material by SiO_2 column chromatography. Yield: 2.9 g (88%). ^{1}H NMR (600 Hz, CD_2Cl_2): δ 2.49 (6 H, s, –CH_3), 2.77 (2 H, dd, J = 8.0 and 6.9 Hz, –NCH_2CH$_2$Ph), 2.85 (2 H, dd, J = 8.0 and 6.9 Hz, –NCH$_2$CH_2Ph), 3.81 (4 H, s, –NCH_2Py), 6.99 (2 H, d, J = 7.6 Hz, $H_{Py\text{-}5}$), 7.12 (2 H, d, J = 7.5 Hz, $H_{Ph\text{-}2}$ and $H_{Ph\text{-}6}$), 7.17 (1 H, t, J = 7.5 Hz, $H_{Ph\text{-}4}$), 7.20 (2 H, d, J = 7.6 Hz, $H_{Py\text{-}3}$), 7.24 (2 H, t, J = 7.5 Hz, $H_{Ph\text{-}3}$ and $H_{Ph\text{-}5}$), 7.48 (2 H, t, J = 7.6 Hz, $H_{Py\text{-}4}$). ^{13}C NMR (600 Hz, CD_2Cl_2): δ 24.53 (–CH_3), 33.86 (–NCH$_2$CH_2Ph), 56.45 (–NCH_2CH$_2$Ph), 60.76 (–NCH_2Py), 119.87 ($C_{Py\text{-}3}$), 121.44 ($C_{Py\text{-}5}$), 126.15 ($C_{Ph\text{-}4}$), 128.51 ($C_{Ph\text{-}3}$ and $C_{Ph\text{-}5}$), 129.28 ($C_{Ph\text{-}2}$ and $C_{Ph\text{-}6}$), 136.75 ($C_{Py\text{-}4}$), 141.22 ($C_{Ph\text{-}1}$), 157.86 ($C_{Py\text{-}6}$), 159.74 ppm ($C_{Py\text{-}2}$). FAB-MS (+); m/z 332.19 (L + H).

***N*,*N*-Bis(6-methylpyridin-2-ylmethyl)-2,2-diphenylethylamine ($\mathbf{L2}^{PhePh}$).** This ligand was prepared by the same procedure described above for the synthesis of $L2^{Phe}$ using 2,2-diphenylethylamine instead of 2-phenylethylamine. Yield: 37%. ^{1}H NMR (600 Hz, CD_2Cl_2): δ 2.50 (6 H, s, –CH_3), 3.18 (2 H, d, J = 7.8 Hz, –NCH_2CHPh$_2$), 3.80 (4 H, s, –NCH_2Py), 4.36 (1 H, t, J = 7.8 Hz, –NCH$_2$CHPh$_2$), 6.89 (2 H, d, J = 7.6 Hz, $H_{Py\text{-}3}$), 6.99 (2 H, d, J = 7.6 Hz, $H_{Py\text{-}5}$), 7.12 (4 H, d, J = 7.2 Hz, $H_{Ph\text{-}2}$ and $H_{Ph\text{-}6}$), 7.19 (2 H, t, J = 7.2 Hz, $H_{Ph\text{-}4}$), 7.25 (4 H, t, J = 7.6 Hz, $H_{Ph\text{-}3}$ and $H_{Ph\text{-}5}$), 7.40 (2 H, t, J = 7.6 Hz, $H_{Py\text{-}4}$). ^{13}C NMR (600 Hz, CD_2Cl_2): δ 24.54 (–CH_3), 49.84 (–NCH$_2$CHPh$_2$), 59.84 (–NCH_2CHPh$_2$), 61.06 (–NCH_2Py), 120.26 ($C_{Py\text{-}3}$), 121.46 ($C_{Py\text{-}5}$), 126.54 ($C_{Ph\text{-}4}$), 128.58 ($C_{Ph\text{-}3}$ and $C_{Ph\text{-}5}$), 128.75 ($C_{Ph\text{-}2}$ and $C_{Ph\text{-}6}$), 136.66 ($C_{Py\text{-}4}$), 144.16 ($C_{Ph\text{-}1}$), 157.71 ($C_{Py\text{-}6}$), 159.37 ppm ($C_{Py\text{-}2}$). FAB-MS (+): m/z 408.2 (L + H).

***N*,*N*-Bis(6-methylpyridin-2-ylmethyl)benzylamine ($\mathbf{L2}^{Bn}$).** This ligand was prepared by the same procedure described above for the synthesis of $L2^{Phe}$ using benzylamine instead of 2-phenylethylamine. Yield: 42%. ^{1}H NMR (400 MHz, $CDCl_3$): δ 2.51 (6 H, s, –CH_3), 3.68 (2 H, s, –CH_2Ph), 3.78 (4 H, s, –CH_2Py), 6.99 (2 H, d, J = 7.5 Hz, $H_{Py\text{-}5}$), 7.19–7.33 (3 H, m, H_{Ph}), 7.42 (2 H, d, J = 7.5 Hz, $H_{Py\text{-}3}$), 7.45 (2 H, d, J = 8.1 Hz, H_{Ph}), 7.55 (2 H, t, J = 7.5 Hz, $H_{Py\text{-}4}$). Anal. Calc. for $C_{21}H_{23}N_3$: C, 79.46; H, 7.30; N, 13.24%. Found: C, 79.49; H, 7.37; N, 13.13%. FAB-MS (+): m/z 318 (L + H). FT-IR/cm^{-1} (KBr disk): 1591 (C=C, aromatic), 1578 (C=C, aromatic).

CAUTION! *The perchlorate salts employed in this study are all potentially explosive and should be handled with care.*

[Cu^I($\mathbf{L2}^{Phe}$)]ClO$_4$ ($\mathbf{2}^{Phe}$). Ligand $L2^{Phe}$ (99.4 mg, 0.3 mmol) was treated with [Cu^I(CH$_3$CN)$_4$]ClO$_4$ (96.1 mg, 0.3 mmol) in CH_2Cl_2 (5 mL) under Ar atmosphere (in a glove box). After stirring for 30 min at room temperature, insoluble materials were removed by filtration. Addition of ether (100 mL) to the filtrate gave a white powder that was precipitated by standing the mixture for several minutes. The supernatant was then removed by decantation, and the remained pale brown solid was washed with ether three times, and dried. Yield: 114 mg (77%). All procedures were done in a glove box (DBO-1KP, Miwa Co. Ltd.) ([O$_2$] < 0.1 ppm). ^{1}H NMR (600 MHz, CD_2Cl_2): δ 2.56 (6 H, s, –CH_3), 2.83 (2 H, t, J = 6.2 Hz, –NCH$_2$CH_2Ph), 3.13 (2 H, d, J = 6.2 Hz, –NCH_2CH$_2$Ph), 3.88 (2 H, d, J = 16.0 Hz, –NCHHPy), 4.20 (2 H, d, J = 16.0 Hz, –NCHHPy), 6.95 (2 H, d, J = 7.3 Hz, $H_{Ph\text{-}2}$ and $H_{Ph\text{-}6}$), 7.24 (2 H, d, J = 7.7 Hz, $H_{Py\text{-}3}$), 7.28 (2 H, d, J = 7.7 Hz, $H_{Py\text{-}5}$), 7.33 (2 H, t, J = 7.3 Hz, $H_{Ph\text{-}3}$ and $H_{Ph\text{-}5}$), 7.43 (1 H, t, J = 7.3 Hz, $H_{Ph\text{-}4}$), 7.75 (2 H, t, J = 7.7 Hz, $H_{Py\text{-}4}$). ^{13}C NMR (600 Hz, CD_2Cl_2): δ 27.36 (–CH_3), 33.94 (–NCH$_2$CH_2Ph), 56.27 (–NCH$_2$CH$_2$Ph), 59.70 (–NCH_2Py), 121.80 ($C_{Py\text{-}3}$), 122.61 ($C_{Ph\text{-}2}$ and $C_{Ph\text{-}6}$), 124.59 ($C_{Py\text{-}5}$), 127.80 ($C_{Ph\text{-}3}$ and $C_{Ph\text{-}5}$), 128.29 ($C_{Ph\text{-}4}$), 138.12 ($C_{Ph\text{-}1}$), 139.27 ($C_{Py\text{-}4}$), 157.26 ($C_{Py\text{-}2}$), 157.94 ppm ($C_{Py\text{-}6}$). FT-IR/cm^{-1} (KBr disk): 1109, 1090 and 625 (ClO_4^-). ESI-MS (+): m/z 394.4 (M^+). Anal. Calc. for $C_{22}H_{26}O_{4.5}N_3CuCl$: C, 52.48; H, 5.21; N, 8.35. Found: C, 52.85; H, 5.05; N, 8.46%.

Table 2 Selected bond lengths (Å) and angles (°) for complexes $\mathbf{2}^{Phe}$, $\mathbf{2}^{PhePh}$, $\mathbf{2}^{Bn}\cdot CH_3CN$ and $\mathbf{2}^{Bn}\cdot CO$

Complex $\mathbf{2}^{Phe}$			
Cu(1)–N(1)	2.202(3)	Cu(1)–N(2)	2.058(3)
Cu(1)–N(3)	2.010(4)	Cu(1)–C(17)	2.627(4)
Cu(1)–C(18)	2.148(4)	Cu(1)–C(19)	2.500(5)
C(17)–C(18)	1.416(7)	C(18)–C(19)	1.416(7)
C(19)–C(20)	1.397(7)	C(20)–C(21)	1.389(7)
C(21)–C(22)	1.379(7)	C(17)–C(22)	1.408(7)
N(1)–Cu(1)–N(2)	81.6(1)	N(1)–Cu(1)–N(3)	84.4(1)
N(2)–Cu(1)–N(3)	116.3(1)	N(1)–Cu(1)–C(18)	96.0(2)
N(2)–Cu(1)–C(18)	103.3(2)	N(3)–Cu(1)–C(18)	139.9(2)
N(1)–Cu(1)–C(19)	129.7(1)	N(2)–Cu(1)–C(19)	111.2(1)
N(3)–Cu(1)–C(19)	124.9(2)	C(18)–Cu(1)–C(19)	34.4(2)
Complex $\mathbf{2}^{PhePh}$			
Cu(1)–N(1)	2.179(6)	Cu(1)–N(2)	1.975(6)
Cu(1)–N(3)	2.051(5)	Cu(1)–C(17)	2.629(7)
Cu(1)–C(18)	2.158(8)	Cu(1)–C(19)	2.441(8)
C(17)–C(18)	1.381(9)	C(17)–C(22)	1.376(9)
C(18)–C(19)	1.40(1)	C(19)–C(20)	1.37(1)
C(20)–C(21)	1.37(1)	C(21)–C(22)	1.38(1)
N(1)–Cu(1)–N(2)	84.8(2)	N(1)–Cu(1)–N(3)	81.3(2)
N(2)–Cu(1)–N(3)	115.6(2)	N(1)–Cu(1)–C(18)	91.2(3)
N(2)–Cu(1)–C(18)	131.8(2)	N(3)–Cu(1)–C(18)	111.1(3)
N(1)–Cu(1)–C(19)	125.9(3)	N(2)–Cu(1)–C(19)	124.3(2)
N(3)–Cu(1)–C(19)	114.4(2)	C(18)–Cu(1)–C(19)	34.9(3)
Complex $\mathbf{2}^{Bn}\cdot CH_3CN$			
Cu(1)–N(1)	2.215(4)	Cu(1)–N(2)	2.050(5)
Cu(1)–N(3)	2.051(5)	Cu(1)–N(4)	1.918(6)
N(1)–Cu(1)–N(2)	80.3(2)	N(1)–Cu(1)–N(3)	82.1(2)
N(1)–Cu(1)–N(4)	119.1(2)	N(2)–Cu(1)–N(3)	115.1(2)
N(2)–Cu(1)–N(4)	120.8(2)	N(3)–Cu(1)–N(4)	122.4(2)
Complex $\mathbf{2}^{Bn}\cdot CO$			
Molecule 1			
Cu(1)–N(1)	2.131(3)	Cu(1)–N(2)	2.042(2)
Cu(1)–N(3)	2.063(3)	Cu(1)–C(22)	1.806(3)
N(1)–Cu(1)–N(2)	83.73(9)	N(1)–Cu(1)–N(3)	80.51(10)
N(1)–Cu(1)–C(22)	127.7(1)	N(2)–Cu(1)–N(3)	105.22(9)
N(2)–Cu(1)–C(22)	129.0(1)	N(3)–Cu(1)–C(22)	117.6(1)
Molecule 2			
Cu(2)–N(4)	2.124(3)	Cu(2)–N(5)	2.054(3)
Cu(2)–N(6)	2.051(3)	Cu(2)–C(44)	1.800(3)
N(4)–Cu(2)–N(5)	83.68(10)	N(4)–Cu(2)–N(6)	80.6(1)
N(4)–Cu(2)–C(44)	129.0(1)	N(5)–Cu(2)–N(6)	108.0(1)
N(5)–Cu(2)–C(44)	121.8(1)	N(6)–Cu(1)–C(44)	122.2(1)

$[Cu^{I}(L2^{PhePh})]ClO_4$ ($\mathbf{2}^{PhePh}$). This compound was prepared in a manner similar to the synthesis of complex $\mathbf{2}^{Phe}$ using ligand $L2^{PhePh}$ (103.6 mg, 0.3 mmol) instead of $L2^{Phe}$. Yield 139 mg (81%). ^{1}H NMR (600 Hz, CD_2Cl_2): δ 2.58 (6 H, s, $-CH_3$), 3.46 (2 H, dd, $J = 8.5$ Hz, $-NCH_2CHPh_2$), 4.05 (2 H, d, $J = 16.2$ Hz, $-NCHHPy$), 4.14 (1 H, t, $J = 8.5$ Hz, $-NCH_2CHPh_2$), 4.36 (2 H, d, $J = 16.2$ Hz, $-NCHHPy$), 7.00 (4 H, dd, $J = 6.3$ and 1.1 Hz, $H_{Ph\text{-}2}$ and $H_{Ph\text{-}6}$), 7.26–7.34 (10 H, m, $H_{Ph\text{-}3}$, $H_{Ph\text{-}4}$, $H_{Ph\text{-}5}$, $H_{Py\text{-}3}$ and $H_{Py\text{-}5}$), 7.81 (t, $J = 7.7$ Hz, $H_{Py\text{-}4}$). ^{13}C NMR (600 Hz, CD_2Cl_2): δ 27.61 ($-CH_3$), 49.87 ($-NCH_2CHPh_2$), 60.95 ($-NCH_2CHPh_2$), 61.20 ($-NCH_2Py$), 121.85 ($C_{Py\text{-}5}$), 124.73 ($C_{Py\text{-}3}$), 125.50 ($C_{Ph\text{-}2}$ and $C_{Ph\text{-}6}$), 128.49 ($C_{Ph\text{-}4}$), 128.64 ($C_{Ph\text{-}3}$ and $C_{Ph\text{-}5}$), 139.57 ($C_{Py\text{-}4}$), 140.81 ($C_{Ph\text{-}1}$), 157.77 ($C_{Py\text{-}2}$), 158.01 ppm ($C_{Py\text{-}6}$). FT-IR/cm^{-1} (KBr disk): 1097 and 623 (ClO_4^-). ESI-MS (+): m/z 470.3 (M^+). Anal. Calc. for $C_{28}H_{30}O_{4.5}N_3CuCl$: C, 58.03; H, 5.22; N, 7.25. Found: C, 58.30; H, 5.09; N, 7.46%.

$[Cu^{I}(L2^{Bn})(CH_3CN)]PF_6$ ($\mathbf{2}^{Bn}\cdot$MeCN). Treatment of ligand $L2^{Bn}$ (0.314 g, 0.99 mmol) and $[Cu^{I}(CH_3CN)_4](ClO_4)$ (0.327 g, 1.00 mmol) in ethanol (20 mL) under anaerobic conditions (in a Schlenk flask) gave a yellow solution, to which an aqueous solution (10 mL) of NH_4PF_6 (0.489 g, 3.00 mmol) was added. The precipitated pale yellow materials were dissolved into the solution again by heating, and the solution was kept standing at room temperature to give yellow crystals. Yield: 0.413 g (72.8%). ^{1}H NMR (400 MHz, acetone-d_6): δ 2.40 (3 H, s, CH_3CN), 2.81 (6 H, s, $-CH_3$), 3.81 (2 H, d (br), $J = 14.9$ Hz, $-NCHHPy$), 4.03 (2 H, s, $-CH_2Ph$), 4.14 (2 H, d (br), $J = 14.9$ Hz, $-NCHHPy$), 7.27–7.36 (5 H, m, H_{Ph} and $H_{Py\text{-}3}$), 7.40 (2 H, d, $J = 7.8$ Hz, H_{Ph}), 7.48 (2 H, m, $H_{Py\text{-}5}$), 7.81 (2H, t, $J = 7.7$ Hz, $H_{Py\text{-}4}$). FT-IR/cm^{-1} (KBr disk): 1603 (C=C, aromatic), 1578, 839 and 557 (PF_6^-). Anal. Calc. for $C_{23}H_{26}N_4CuPF_6$: C, 48.72; H, 4.62; N, 9.88. Found: C, 48.62; H, 4.64; N, 9.89%.

$[Cu^{I}(L2^{Bn})(CH_3CN)]ClO_4$ was prepared similarly but without the salt exchange reaction with NH_4PF_6. Yield: 82%. FT-IR/cm^{-1} (KBr disk): 1603 (C=C, aromatic), 1576, 1086, 794 and 623 (ClO_4^-). FAB-MS (+): m/z 380 (M^+). Anal. Calc. for $C_{23}H_{26}N_4O_4CuCl$: C, 52.97; H, 5.03; N, 10.74. Found: C, 52.64; H, 4.99; N, 10.77%.

$[Cu^{I}(L2^{Bn})(CO)]PF_6$ ($\mathbf{2}^{Bn}\cdot$CO). Treatment of $[Cu^{I}(L2^{Bn})(CH_3CN)]PF_6$ (1.14 g, 2.01 mmol) in ethanol (4 mL) under CO atmosphere over night gave white powder which was collected by filtration. Yield: 1.04 g (93.0%). ^{1}H NMR (400 MHz, acetone-d_6): δ 2.85 (6 H, s, $-CH_3$), 3.99 (2 H, d, $J = 15.9$ Hz, $-CHHPy$), 4.31 (2 H, s, $-CH_2Ph$), 4.47 (2 H, d, $J = 15.9$ Hz, $-CHHPy$), 7.31–7.40 (5 H, m, H_{Ph} and $H_{Py\text{-}3}$), 7.49 (2 H, d, $J = 7.8$ Hz, H_{Ph}), 7.54 (2 H, m, $H_{Py\text{-}5}$), 7.90 (2 H, t, $J = 7.7$ Hz, $H_{Py\text{-}4}$). FT-IR/cm^{-1} (KBr disk): 2088 and 2100 (C≡O), 1606 (C=C, aromatic), 1578, 841 and 557 (PF_6^-). Anal. Calc. for $C_{22}H_{23}N_3OCuPF_6$: C, 47.70; H, 4.19; N, 7.59. Found: C, 47.75; H, 4.16; N, 7.60%.

Single crystals of the copper(I) complex with ClO_4^- counter anion, $[Cu^{I}(L2^{Bn})(CO)]ClO_4$, were obtained by the same treatment of $[Cu^{I}(L2^{Bn})(CH_3CN)]ClO_4$ with CO in a 81% yield. FT-IR/cm^{-1} (KBr disk): 2096 and 2085 (CO), 1606 (C=C, aromatic), 1578, 1091, 791 and 623 (ClO_4^-). Anal. Calc. for $C_{22}H_{23}N_3O_5CuCl$: C, 51.97; H, 4.56; N, 8.26. Found: C, 51.73; H, 4.52; N, 8.43%.

$[Cu^{I}(L2^{Bn})]PF_6$ ($\mathbf{2}^{Bn}$). This complex was prepared by removing CO from $[Cu^{I}(L2^{Bn})(CO)]PF_6$. Thus, a methanol solution of the CO-complex was heated on hot water-bath (75 °C) for 10 min, and then the solvent was removed under reduced pressure to give yellow powder of $\mathbf{2}^{Bn}$. ^{1}H NMR (400 MHz, acetone-d_6): δ 2.83 (6 H, s, $-CH_3$), 3.97 (2 H, s, $-CH_2Ph$), 3.8–4.3 (4 H, br s, $-CH_2Py$), 7.25–7.37 (7 H, m, H_{Ph} and $H_{Py\text{-}3}$), 7.45 (2 H, d, $J = 7.7$ Hz, $H_{Py\text{-}5}$), 7.86 (2 H, t, $J = 7.7$ Hz, $H_{Py\text{-}4}$). FT-IR/cm^{-1} (KBr disk): 1610 (C=C, aromatic), 1577, 849 and 557 (PF_6^-). EI-MS (CH_2Cl_2): m/z 380.1 (M^+). A satisfactory result of elemental analysis could not be obtained due to instability of the complex.

Results and discussion

Characterization of copper(I) complexes

The tridentate ligands [$L2^R$; R = $-CH_2Ph$ (Bn), $-CH_2CH_2Ph$ (Phe) and $-CH_2CHPh_2$ (PhePh)] were prepared by reductive coupling of the corresponding amines (RNH_2) and 2 equiv of 6-methyl-2-pyridinecarbaldehyde in the presence of $NaBH_3CN$ as the reductant. Treatment of the ligand with an equimolar amount of $[Cu^{I}(CH_3CN)_4]ClO_4$ under anaerobic conditions (Ar) gave the corresponding copper(I) complexes $\mathbf{2}^R$ as ClO_4^- salts. In the case of $\mathbf{2}^{Bn}$, single crystals of the CH_3CN-containing complex, $\mathbf{2}^{Bn}\cdot CH_3CN$, were obtained as a PF_6^- salt which was prepared by the salt exchange reaction of the ClO_4^--complex

with NH_4PF_6. $\mathbf{2}^{Bn}\cdot CH_3CN$ can be easily converted into air-stable carbonyl complex $\mathbf{2}^{Bn}\cdot CO$ by treating it with CO gas. Furthermore, the CO ligand in $\mathbf{2}^{Bn}\cdot CO$ can be easily removed by heating it at 75 °C for 10 min to give complex $\mathbf{2}^{Bn}$ without any external ligand. Crystal structures of $[Cu^{I}(L2^{Phe})]ClO_4$ ($\mathbf{2}^{Phe}$), $[Cu^{I}(L2^{PhePh})]ClO_4$ ($\mathbf{2}^{PhePh}$), $[Cu^{I}(L2^{Bn})(CH_3CN)]PF_6$ ($\mathbf{2}^{Bn}\cdot CH_3CN$) and $[Cu^{I}(L2^{Bn})(CO)]ClO_4$ ($\mathbf{2}^{Bn}\cdot CO$) have been determined by X-ray crystallographic analysis as shown in Fig. 1. The crystallographic data of the complexes are presented in Table 1, and their selected bond lengths and angles around the copper ion are summarized in Table 2.

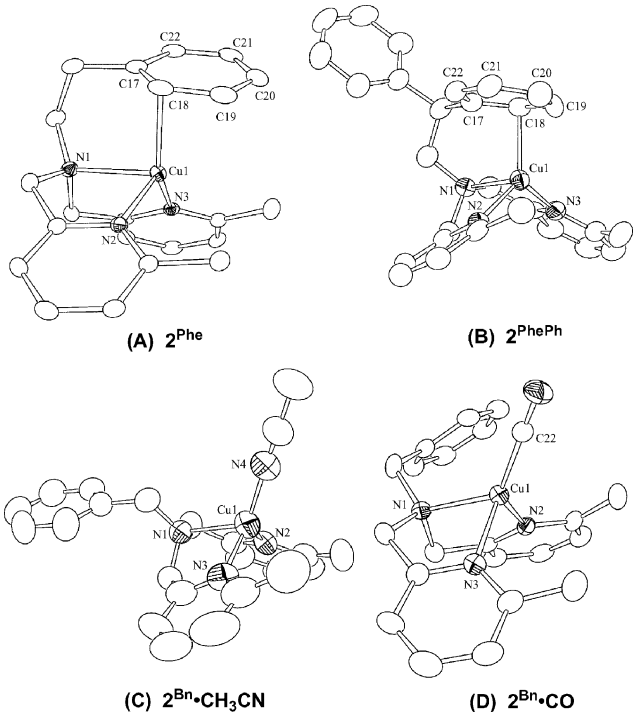

Fig. 1 ORTEP drawings of (A) $[Cu^{I}(L2^{Phe})]ClO_4$ ($\mathbf{2}^{Phe}$), (B) $[Cu^{I}(L2^{PhePh})]ClO_4$ ($\mathbf{2}^{PhePh}$), (C) $[Cu^{I}(L2^{Bn})(CH_3CN)]PF_6$ ($\mathbf{2}^{Bn}\cdot CH_3CN$) and (D) $[Cu^{I}(L2^{Bn})(CO)]ClO_4$ $\mathbf{2}^{Bn}\cdot CH_3CN$) showing 50% probability thermal ellipsoids. The counter anion and hydrogen atoms are omitted for clarity.

d–π Interaction in $\mathbf{2}^{R}$. Copper(I) complexes $\mathbf{2}^{Phe}$ and $\mathbf{2}^{PhePh}$ containing $-CH_2CH_2Ph$ (Phe) and $-CH_2CHPh_2$ (PhePh) sidearms, respectively, exhibit a copper(I)–arene interaction in the crystals, where the phenyl ring of the *N*-alkyl substituent (ligand sidearm) exists just above the cuprous ion as shown in Fig. 1(A) and (B), respectively. The cuprous ion of each complex adapts to a trigonal pyramidal geometry consisting of the two pyridine nitrogen atoms N(2) and N(3) and one of the *ortho*-carbon atoms C(18) of the phenyl ring occupying the trigonal basal plane and the tertiary alkyl amine nitrogen atom N(1) as the axial ligand. Deviation of the copper(I) ion from the basal plane is 0.076 and 0.163 Å in $\mathbf{2}^{Phe}$ and $\mathbf{2}^{PhePh}$, respectively. It should be noted that the distances between Cu and C(18) (2.148 Å in $\mathbf{2}^{Phe}$ and 2.165 Å in $\mathbf{2}^{PhePh}$) are much shorter than the Cu–C(17) distances (2.629 Å in $\mathbf{2}^{Phe}$ and 2.639 Å in $\mathbf{2}^{PhePh}$). Thus, the copper(I)–arene interaction in these complexes can be described as an η^1-binding interaction.

We have already demonstrated that copper(I) complexes $\mathbf{1}^{R}$ (R = $-CH_2CH(X)Ph$ where X = H, Me and Ph) supported by bis[2-(pyridin-2-yl)ethyl]amine tridentate ligands $L1^{R}$ with the longer ethylene linker exhibit a distorted tetrahedral geometry involving a d–π interaction with an η^2-binding mode, while complex $\mathbf{3}^{Phe}$ with bis(pyridin-2-ylmethyl)amine ligand $L3^{Phe}$ shows a trigonal pyramidal structure involving a d–π interaction with an η^1-binding mode as illustrated in Fig. 2.[11,18,20] Thus, the copper(I)–arene interaction in $\mathbf{2}^{R}$ resembles that in complex $\mathbf{3}^{Phe}$.

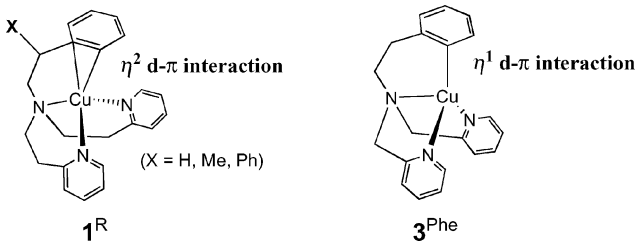

Fig. 2 d–π Interaction in complexes $\mathbf{1}^{R}$ and $\mathbf{3}^{Phe}$.

In fact, the distances from the copper(I) ion to the aromatic carbon atom and to the ligand nitrogen atoms in $\mathbf{2}^{Phe}$ and $\mathbf{2}^{PhePh}$ are similar to those in $\mathbf{3}^{Phe}$.

In the UV-vis spectra, copper(I) complexes $\mathbf{2}^{Phe}$ and $\mathbf{2}^{PhePh}$ exhibit a characteristic absorption band around 270 nm (Table 3), which has been tentatively assigned to an MLCT (metal-to-ligand charge transfer) band through the d–π interaction as in the case of other copper(I) complexes exhibiting a d–π interaction.[11,18,20,21] The relative strength of the d–π interaction can be evaluated by the competitive binding of CH_3CN to the cuprous ion (titration of $\mathbf{2}^{R}$ by CH_3CN) in a non-polar solvent such as CH_2Cl_2.[11,18,20] The MLCT band around 270 nm gradually decreased, when CH_3CN was added into a CH_2Cl_2 solution of $\mathbf{2}^{R}$. Fig. S1 (ESI‡) shows the spectral change for the titration of complex $\mathbf{2}^{Phe}$ by CH_3CN in CH_2Cl_2 at −20 °C as a typical example. A decrease of the absorption band around 270 nm may be due to the ligand exchange reaction between the phenyl ring of the d–π interaction and the added CH_3CN. The association constant of CH_3CN to the copper(I) ion of $\mathbf{2}^{Phe}$, $K_{as} = [Cu^{I}L(CH_3CN)]/[Cu^{I}L][CH_3CN]$, was then determined as $622 \pm 15\ M^{-1}$ by analyzing the absorption change as indicated in the inset of Fig. S1, and the K_{as} values for $\mathbf{2}^{PhePh}$ and $\mathbf{2}^{Bn}$ were determined similarly, as listed in Table 3, where the K_{as} values for $\mathbf{1}^{Phe}$ and $\mathbf{3}^{Phe}$ are also included.

The K_{as} value may reflect the strength of the d–π interaction in the copper(I) complexes. Namely, the smaller the K_{as} value (thus the weaker the CH_3CN-binding), the stronger the d–π interaction. As clearly seen in Table 3, the K_{as} values of $\mathbf{2}^{Phe}$ and $\mathbf{2}^{PhePh}$ are much larger than that of $\mathbf{1}^{Phe}$ having the η^2-binding interaction, but are smaller than that of $\mathbf{3}^{Phe}$. Thus, the strength of d–π interaction decreases in the order of $\mathbf{1}^{Phe} > \mathbf{2}^{R} > \mathbf{3}^{Phe}$ (the strength of d–π interaction in $\mathbf{2}^{Bn}$ is discussed below). Although the theoretical aspects of the d–π interaction have yet to be addressed in detail, the order of strength of the d–π interaction seems to be correlated to the order of the electron-donor ability of ligand; $\mathbf{1}^{R} < \mathbf{2}^{R} < \mathbf{3}^{R}$ (the order of electron-donor ability of pyridine is discussed below). Namely, the d–π interaction becomes stronger ($\mathbf{1}^{R} > \mathbf{2}^{R} > \mathbf{3}^{R}$) as the electron-donor ability of ligands becomes weaker ($\mathbf{1}^{R} < \mathbf{2}^{R} < \mathbf{3}^{R}$). In other words, the d–π interaction becomes stronger ($\mathbf{1}^{R} > \mathbf{2}^{R} > \mathbf{3}^{R}$) as the bonding interaction between the cuprous ion and the pyridine nitrogen becomes weaker ($\mathbf{1}^{R} < \mathbf{2}^{R} < \mathbf{3}^{R}$). On the other hand, the meaningful difference in K_{as} between $\mathbf{2}^{Phe}$ and $\mathbf{2}^{PhePh}$ can be attributed to a steric effect of the benzylic substituent (Ph) in

Table 3 The UV-vis data and the equilibrium constants K_{as} for the titration of copper(I) complexes with CH_3CN in CH_2Cl_2[a]

Complex	λ_{max}/nm (ε/M^{-1} cm^{-1})	K_{as}/M^{-1}
$\mathbf{1}^{Phe}$[b]	290 (8820)	6.4 ± 0.1
$\mathbf{2}^{Phe}$	270 (13500)	622 ± 15
$\mathbf{2}^{PhePh}$	270 (13100)	230 ± 6.0
$\mathbf{2}^{Bn}$	285 (20900)[d]	4470 ± 330
$\mathbf{3}^{Phe}$[c]	290 (6010)	3360 ± 17

[a] At −20 °C. [b] The data were taken from the literature.[20] [c] The data were taken from the literature.[11] [d] Shoulder.

$\mathbf{2}^{PhePh}$, which prohibits free rotation of the ligand sidearm, thus stabilizing the d–π interaction.[20]

Copper(I) complexes of L2^{Bn}. Crystal structures of $\mathbf{2}^{Bn}\cdot CH_3CN$ and $\mathbf{2}^{Bn}\cdot CO$ are shown in Fig. 1(C) and (D), respectively. Copper(I) complex $\mathbf{2}^{Bn}\cdot CH_3CN$ exhibits a distorted trigonal pyramidal structure with an N_4 donor set, where two pyridine nitrogen atoms N(2) and N(3) and acetonitrile nitrogen N(4) occupy the trigonal basal plane and tertiary amine nitrogen N(1) acts as an axial ligand. The axial ligand N(1), however, largely slips out of the ideal position of the apex of trigonal pyramidal geometry. Apparently, there is no interaction between the cuprous ion and the phenyl group of the ligand sidearm ($-CH_2Ph$) in $\mathbf{2}^{Bn}\cdot CH_3CN$.

The unit cell of copper(I) complex $\mathbf{2}^{Bn}\cdot CO$ consists of two crystallographically independent molecules. Both of the cuprous centers of $\mathbf{2}^{Bn}\cdot CO$ also have a distorted trigonal pyramidal (or a significantly distorted tetrahedral) geometry where CH_3CN ligand in $\mathbf{2}^{Bn}\cdot CH_3CN$ is replaced by a CO molecule. In this complex as well, there is no d–π interaction between the metal center and the phenyl group of the *N*-benzyl substituent.

The CO ligand in $\mathbf{2}^{Bn}\cdot CO$ can be easily removed by heating it in methanol to give $\mathbf{2}^{Bn}$ involving no external ligand. Although structural examination of $\mathbf{2}^{Bn}$ has yet to be accomplished due to its instability in solution, complex $\mathbf{2}^{Bn}$ exhibits a shoulder absorption band at 285 nm in CH_2Cl_2. This absorption band disappeared when acetonitrile was added into the solution of $\mathbf{2}^{Bn}$, and the final spectrum of the titration was identical to that of $\mathbf{2}^{Bn}\cdot CH_3CN$ [λ_{max} = 313 nm (ε = 7700 M^{-1} cm^{-1})]. Thus, the 285 nm band of $\mathbf{2}^{Bn}$ can be also attributed to a MLCT transition of a d–π interaction, although the binding mode of copper(I) to the phenyl group is not clear at present. As clearly seen in Table 3, the K_{as} value of $\mathbf{2}^{Bn}$ is significantly larger than those of $\mathbf{2}^{R}$ (R = Phe and PhePh) and fairly close to that of $\mathbf{3}^{Phe}$. This means that the d–π interaction in $\mathbf{2}^{Bn}$ is much weaker than that in $\mathbf{2}^{Phe}$ and $\mathbf{2}^{PhePh}$ and is comparable to that in $\mathbf{3}^{Phe}$. The weaker interaction could be attributed to the shorter methylene linker between the amine nitrogen atom and the phenyl ring of the ligand sidearm. Namely, the methylene linker may be too short to construct a stable d–π interaction.

Redox potentials of the copper(I) complexes. Copper(I) complexes $\mathbf{2}^{Phe}$ and $\mathbf{2}^{PhePh}$ exhibited a quasi-reversible redox couple due to one-electron oxidation–reduction of the copper center in CH_2Cl_2. The redox potentials ($E_{1/2}$ *vs.* Fc/Fc^+) of these complexes are listed in Table 4 together with those of $\mathbf{1}^{Phe}$ and $\mathbf{3}^{Phe}$. The redox behavior of $\mathbf{2}^{Bn}$ was not so simple probably due to instability of the complex under the present experimental conditions.

As clearly seen in Table 4, the $E_{1/2}$ values of $\mathbf{1}^{Phe}$, $\mathbf{2}^{Phe}$ and $\mathbf{3}^{Phe}$ decrease in this order ($E_{1/2}$ = 0.07, −0.06 and −0.20 V *vs.* Fc/Fc^+, respectively). The higher $E_{1/2}$ value of $\mathbf{1}^{Phe}$ has been attributed to the lower electron-donor ability of pyridine of ligand $L1^{Phe}$ as compared to that of other ligands, which can be simply attributed to the chelate ring size effect that is normally in the order of six-membered ring < five-membered ring.[12] Then, it becomes apparent that the 6-methyl group in $\mathbf{2}^{Phe}$ somewhat reduces the electron-donor ability of pyridine to cause the negative shift of $E_{1/2}$ as compared to that of $\mathbf{3}^{Phe}$. However, the electron-donor ability of pyridine in $\mathbf{2}^{Phe}$ is still higher than that in $\mathbf{1}^{Phe}$, making the order of $E_{1/2}$ as $\mathbf{1}^{Phe} > \mathbf{2}^{Phe} > \mathbf{3}^{Phe}$. The fact that the $E_{1/2}$ value of $\mathbf{2}^{PhePh}$ is somewhat higher than that of $\mathbf{2}^{Phe}$ suggests that the stronger d–π interaction stabilizes the lower oxidation state of copper(I) more than the copper(II) oxidation state. A similar trend was seen in the $\mathbf{1}^{R}$ system, where the $E_{1/2}$ value of $\mathbf{1}^{PhePh}$ is higher than that of $\mathbf{1}^{Phe}$ ($\Delta E_{1/2}$ = 0.08 V).[20]

Copper(I)–dioxygen reactivity

Ligand effects on the copper(I)–dioxygen reactivity were also examined. As noted in Introduction, the copper(I) complexes of $L1^{R}$-type ligands ($\mathbf{1}^{R}$) mainly afford (μ-η^2:η^2-peroxo)dicopper(II) complex **A** in the reaction with O_2 at a low temperature, whereas the copper(I) complex of $L3^{R}$ ($\mathbf{3}^{R}$) predominantly affords bis(μ-oxo)dicopper(III) complex **B** in a similar reaction. Thus, it is of interest to know what is obtained in the oxygenation reaction of $\mathbf{2}^{R}$.

Treatment of copper(I) complexes $\mathbf{2}^{Phe}$ with O_2 in anhydrous acetone at −80 °C readily afforded a brown solution which exhibited an intense absorption band at 355 nm (ε = 18700 M^{-1} cm^{-1}) together with a relatively weak band at 511 nm (770 M^{-1} cm^{-1}) as shown in Fig. 3. Similar spectra were obtained in the reaction of $\mathbf{2}^{PhePh}$ and $\mathbf{2}^{Bn}$ under the same experimental conditions (see Table 4 and Fig. 4). After a short lag phase (0–10 s), the reaction obeys second-order kinetics, and the second-order rate constant (k_{obs}) was obtained from the slope of the line of the second-order plot shown in the

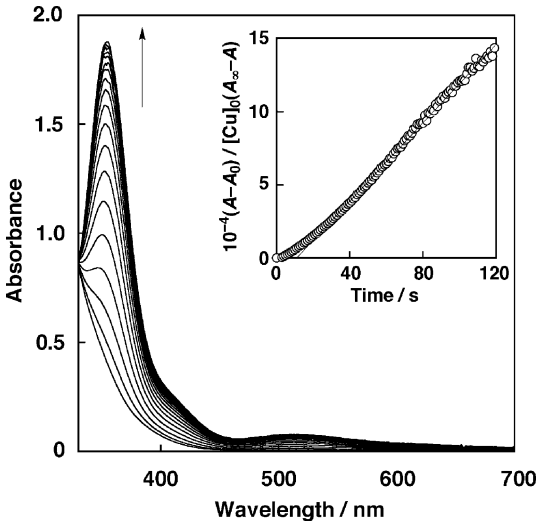

Fig. 3 Spectral change observed upon introduction of O_2 gas into acetone solution of $\mathbf{2}^{Phe}$ (2.0×10^{-4} M) at −80 °C. Inset: second-order plot based on the absorption change at 355 nm.

Table 4 Redox potentials ($E_{1/2}$)[a] of the copper(I) complexes, UV-vis and resonance Raman data of the Cu_2/O_2 complexes and second-order rate constants (k_{obs}) for the formation of Cu_2/O_2 complexes at −80 °C in acetone

		Cu_2/O_2 complex		
Complex	$E_{1/2}$, V *vs.* Fc/Fc^+[a]	UV-vis, λ_{max}/nm (ε/M^{-1} cm^{-1})	Raman, $\nu_{O\text{-}O}$ ($\Delta\nu_{^{16}O\text{-}^{18}O}$)	Formation rate, k_{obs}/M^{-1} s^{-1}
$\mathbf{1}^{Phe}$[b]	0.07	362 (15400) ~520 (770)	746 (42)	4.1
$\mathbf{2}^{Phe}$	−0.06	355 (18700) 511 (770)	726 (36)	130.0
$\mathbf{2}^{PhePh}$	0.01	356 (16700) ~505 (770)	716 (37)	33.6
$\mathbf{2}^{Bn}$	—	353 (23500) 529 (970)	714 (39)	29.2
$\mathbf{3}^{Phe}$[c]	−0.20	385 (6540)	—	59000[d]

[a] The electrochemical measurements were performed in CH_2Cl_2 containing 0.1 M tetrabutylammonium perchlorate (TBAP) at a scan rate of 10–50 mV s^{-1} at 25 °C. [b] The data are taken from the literature.[20] [c] The data are taken from the literature.[11] [d] At −94 °C in acetone.

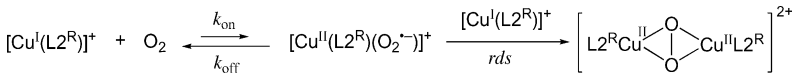

Scheme 1

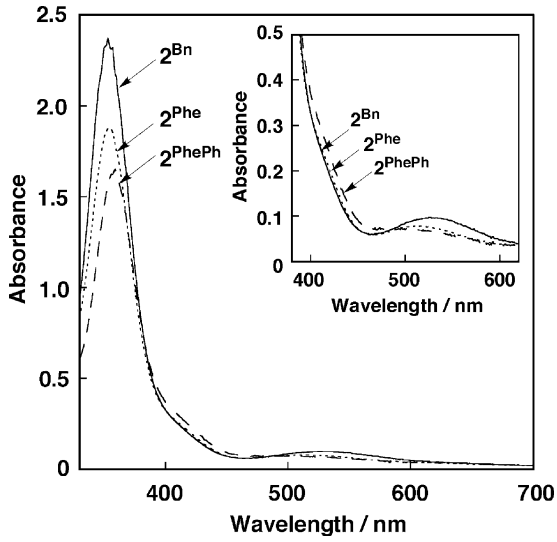

Fig. 4 Absorption spectra of the oxygenated products of $\mathbf{2}^{Phe}$, $\mathbf{2}^{PhePh}$ and $\mathbf{2}^{Bn}$ in acetone at −80 °C. The initial concentration of $\mathbf{2}^{Phe}$, $\mathbf{2}^{PhePh}$ and $\mathbf{2}^{Bn}$ is 2.0×10^{-4} M.

inset of Fig. 3. The second-order kinetics clearly indicates that two molecules of the copper complex are involved in the rate-determining step of the Cu_2/O_2 complex formation process. It can be presumed that the bimolecular reaction between a mononuclear (superoxo)copper(II) complex, generated by the reaction of $\mathbf{2}^{R}$ and O_2, and another molecule of copper(I) complex is the rate-determining step as indicated in Scheme 1. The initial lag phase shown in Fig. 3 may be due to the time required to attain the pre-equilibrium reaction between the copper(I) complex and O_2 to give the (superoxo)copper(II) intermediate (see Scheme 1). From the dependence of the rate constants on the reaction temperature shown as Arrhenius plots in Fig. S2 (ESI‡) were obtained the activation enthalpy ($\Delta H^{\neq}$) of 5.8 ± 0.3 and 8.2 ± 0.3 kJ mol^{-1} and the activation entropy ($\Delta S^{\neq}$) of −140.1 ± 1.6 and −139.1 ± 1.5 J K^{-1} mol^{-1} for the oxygenation reaction of $\mathbf{2}^{Phe}$ and $\mathbf{2}^{PhePh}$, respectively. The significantly large negative $\Delta S^{\neq}$ values are consistent with the proposed mechanism (Scheme 1), where the bimolecular reaction between the monomeric (superoxo)copper(II) complex, $[Cu^{II}(L2^{R})(O_2^{\bullet-})]^+$, and another Cu(I) starting compound is the rate determining step.[22]

In all cases, frozen CH_2Cl_2 solutions of the oxygenated product were ESR silent at −150 °C. The UV-vis features shown in Fig. 4 as well as the ESR silence strongly suggest that the oxygenated product is (μ-η^2:η^2-peroxo)dicopper(II) complex **A**. It should be noted, however, that intensity of the LMCT bands at ~355 and ~510 nm due to the side-on peroxo complex **A** is somewhat different among the three ligand systems $L2^{R}$ (R = Bn, Phe and PhePh, decreasing in this order) and the shoulder ~400 nm seems to grow in going from $L2^{Bn}$ to $L2^{PhePh}$. The spectral feature around 400 nm can be attributed to co-existence of a bis(μ-oxo)dicopper(III) complex **B**. This was confirmed by the resonance-Raman studies described below.

Fig. 5 shows the resonance-Raman spectra of the oxygenated product of $\mathbf{2}^{Bn}$, $\mathbf{2}^{Phe}$ and $\mathbf{2}^{PhePh}$ obtained with 514.5 nm excitation in acetone at –90 °C. In all cases, a relatively intense Raman band at 714–726 cm^{-1} with an isotope shift of 36–39 cm^{-1} with $^{18}O_2$ was obtained. These Raman features have been ascribed to the O–O bond stretching vibration of the side-on peroxo ligand.[23] Thus, the data unambiguously support the formation of (μ-η^2:η^2-

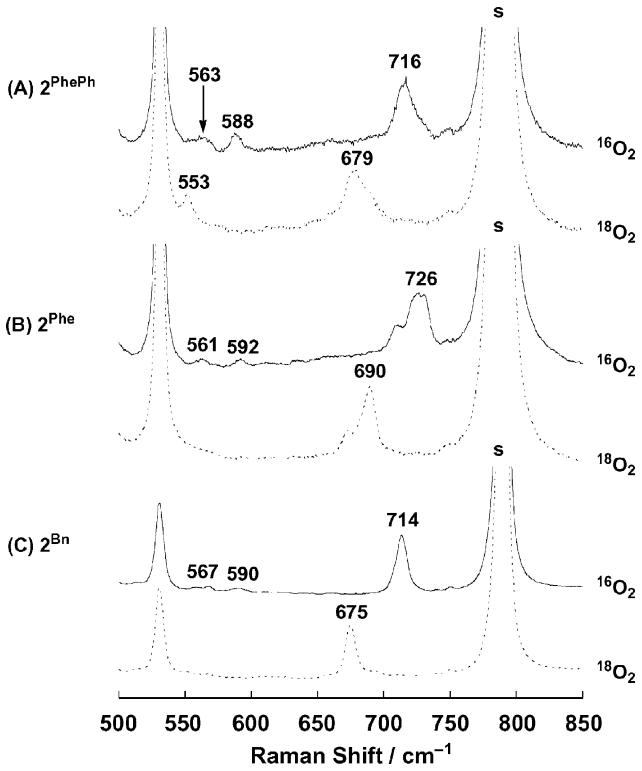

Fig. 5 Resonance Raman spectra of the oxygenated products of (A) $\mathbf{2}^{PhePh}$, (B) $\mathbf{2}^{Phe}$ and (C) $\mathbf{2}^{Bn}$ obtained with 514.5 nm excitation in acetone at −90 °C. The label 's' denotes the solvent peak.

peroxo)dicopper(II) complex **A**. In addition, Cu–Cu stretching vibrations in the (μ-η^2:η^2-peroxo)dicopper(II) core were observed at 312 and 280 cm^{-1} for $\mathbf{2}^{PhePh}$ and 314 and 282 cm^{-1} for $\mathbf{2}^{Phe}$ (data not shown in Fig. 5), further confirming the formation of side-on peroxo dicopper(II) complex **A**.[24]§ Notably, the frequency of the O–O bond stretching vibration of **A** supported by $L2^{R}$ (714–726 cm^{-1}) is relatively lower than that of the $L1^{Phe}$-complex (746 cm^{-1}, see Table 4). The results clearly suggest that the O–O bond in the $L2^{R}$-complexes is relatively weakened as compared to that in the $L1^{R}$-complex. This could be also attributed to the higher electron-donor ability of pyridine in $L2^{R}$ as compared to $L1^{R}$, as discussed below.

As stated above, the UV-vis spectra (Fig. 4) suggested co-existence of bis(μ-oxo)dicopper(III) complex **B** in solution. This was confirmed by the resonance Raman data. Namely, weak Raman bands due to bis(μ-oxo)dicopper(III) complex **B** were detected at 588 and 563 cm^{-1} (Fermi doublet) for $\mathbf{2}^{PhePh}$, 592 and 561 cm^{-1} for $\mathbf{2}^{Phe}$, and 590 and 567 cm^{-1} for $\mathbf{2}^{Bn}$. The Fermi doublet signals of $\mathbf{2}^{PhePh}$ in the $^{16}O_2$-derivative shift into one band at 553 cm^{-1}. Thus, the isotope shift was calculated to be 23 cm^{-1} by subtracting the frequency (553 cm^{-1}) of the $^{18}O_2$-derivative from the average frequency (578 cm^{-1}) of the $^{16}O_2$-derivative. These results are consistent with the well-established Raman data of the bis(μ-oxo)dicopper(III) complexes.[25] It is also apparent that the content of bis(μ-oxo)dicopper(III) complex **B** increases in going from $\mathbf{2}^{Bn}$ to $\mathbf{2}^{PhePh}$. Thus, the Raman peaks of the $^{18}O_2$-derivatives derived from $\mathbf{2}^{Bn}$ and $\mathbf{2}^{Phe}$ were too weak to be detected (see Fig. 5 (B) and (C)). These results are also consistent with the UV-vis data shown in Fig. 4,

§ In the reaction of $\mathbf{2}^{Bn}$, the Cu–Cu stretching vibration was not detected, the reason for which is not clear at present.

where content of the bis(μ-oxo)dicopper(III) species somewhat increases in going from $\mathbf{2}^{Bn}$ to $\mathbf{2}^{PhePh}$, although the reason for this phenomenon is not clear at present. There could be some sort of interaction between copper(III) ion in **B** and the aromatic group of the ligand sidearm of $\mathbf{2}^{PhePh}$, somewhat stabilizing the bis(μ-oxo)dicopper(III) species.

Consequently, copper(I) complexes $\mathbf{2}^{R}$ have been demonstrated to afford mainly the side-on peroxo dicopper(II) complex **A** in the reaction with O_2 at the low temperature. This clearly demonstrates that the introduction of the 6-methyl group into the pyridylmethylamine tridentate ligand $L3^{R}$ leading to $L2^{R}$ resulted in a drastic change in the structure of Cu_2/O_2 complex from bis(μ-oxo)dicopper(III) **B** to (μ-η^2:η^2-peroxo)dicopper(II) **A**. The result can be explained by taking account of the decreased electron-donor ability of pyridine of $L2^{R}$ due to the steric repulsion between the bound metal ion and the 6-methyl substituent. Ligand $L2^{R}$, with the lower donor ability, may not be able to stabilize the higher oxidation state of copper(III) in **B**, thus providing the side-on peroxo complex **A** with the copper(II) oxidation state as the major product. Thus, the electronic effect of $L2^{R}$ seems to be closer to that of $L1^{R}$; both ligands afford the (μ-η^2:η^2-peroxo)dicopper(II) complex **A**. Nonetheless, the strength of the O–O bond of the side-on peroxo ligand in the $L2^{R}$-complex is weakened as compared to the O–O bond strength of the $L1^{R}$-complex as evident from the lower $\nu_{O\text{-}O}$ value of the former (Table 4).

Reactivity differences in the Cu_2/O_2-formation process (rate constant k_{obs} in Table 4) evidences the ligand effects more clearly. Namely, $\mathbf{3}^{Phe}$ supported by the ligand with the highest electron-donor ability reacted with O_2 more than 10^4-fold faster than $\mathbf{1}^{Phe}$ with the ligand having the lowest electron-donor ability, whereas the reactivity of $\mathbf{2}^{R}$ lay in between.

In summary, the structure and reactivity of copper(I) complexes supported by pyridylalkylamine tridentate ligands can be finely tuned not only by changing the alkyl linker chain length between the pyridine nucleus and tertiary amine nitrogen but also by introducing a methyl substituent at the 6-position of the pyridine donor group. Further studies on the reactivity of peroxo complexes supported by $L2^{R}$-type ligands toward external substrates are now under progress.

Acknowledgements

This work was financially supported in part by Grants-in-Aid for Scientific Research (No. 15350105 for S. I. and No. 16350030 for M. S.) from the Ministry of Education, Culture, Sports, Science and Technology, Japan and by Research Fellowships of Japan Society for the Promotion of Science for Young Scientists.

References

1 K. D. Karlin, S. Kaderli and A. D. Zuberbühler, *Acc. Chem. Res.*, 1997, **30**, 139–147.
2 S. Itoh and S. Fukuzumi, *Bull. Chem. Soc. Jpn.*, 2002, **75**, 2081–2095.
3 L. M. Mirica, X. Ottenwaelder and T. D. P. Stack, *Chem. Rev.*, 2004, **104**, 1013–1045.
4 E. A. Lewis and W. B. Tolman, *Chem. Rev.*, 2004, **104**, 1047–1076.
5 M. Suzuki, H. Furutachi and H. Okawa, *Coord. Chem. Rev.*, 2000, **200**, 105–129.
6 K. D. Karlin, M. S. Haka, R. W. Cruse, G. J. Meyer, A. Farooq, Y. Gultneh, J. C. Hayes and J. Zubieta, *J. Am. Chem. Soc.*, 1988, **110**, 1196–1207.
7 K. D. Karlin, J. C. Hayes, Y. Gultneh, R. W. Cruse, J. W. McKown, J. P. Hutchinson and J. Zubieta, *J. Am. Chem. Soc.*, 1984, **106**, 2121–2128.
8 E. Pidcock, H. V. Obias, M. Abe, H.-C. Liang, K. D. Karlin and E. I. Solomon, *J. Am. Chem. Soc.*, 1999, **121**, 1299–1308.
9 E. Pidcock, H. V. Obias, C. X. Zhang, K. D. Karlin and E. I. Solomon, *J. Am. Chem. Soc.*, 1998, **120**, 7841–7847.
10 S. Itoh, H. Kumei, M. Taki, S. Nagatomo, T. Kitagawa and S. Fukuzumi, *J. Am. Chem. Soc.*, 2001, **123**, 6708–6709.
11 T. Osako, Y. Ueno, Y. Tachi and S. Itoh, *Inorg. Chem.*, 2003, **42**, 8087–8097.
12 K. D. Karlin and S. E. Sherman, *Inorg. Chim. Acta*, 1982, **65**, L39–L40.
13 M. J. Henson, M. A. Vance, C. X. Zhang, H.-C. Liang, K. D. Karlin and E. I. Solomon, *J. Am. Chem. Soc.*, 2003, **125**, 5186–5192.
14 H. Hayashi, S. Fujinami, S. Nagatomo, S. Ogo, M. Suzuki, A. Uehara, Y. Watanabe and T. Kitagawa, *J. Am. Chem. Soc.*, 2000, **122**, 2124–2125.
15 H. Hayashi, K. Uozumi, S. Fujinami, S. Nagatomo, K. Shiren, H. Furutachi, M. Suzuki, A. Uehara and T. Kitagawa, *Chem. Lett.*, 2002, 416–417.
16 M. Costas, M. P. Mehn, M. P. Jensen and L. Que, Jr., *Chem. Rev.*, 2004, **104**, 939–986.
17 H. Nagao, N. Komeda, M. Mukaida, M. Suzuki and K. Tanaka, *Inorg. Chem.*, 1996, **35**, 6809–6815.
18 T. Osako, Y. Tachi, M. Taki, S. Fukuzumi and S. Itoh, *Inorg. Chem.*, 2001, **40**, 6604–6609.
19 D. D. Perrin, W. L. F. Armarego and D. R. Perrin, *Purification of Laboratory Chemicals*, Pergamon Press, Elmsford, NY, 4th edn., 1996.
20 T. Osako, Y. Tachi, M. Doe, M. Shiro, K. Ohkubo, S. Fukuzumi and S. Itoh, *Chem. Eur. J.*, 2004, **10**, 237–246.
21 Y. Shimazaki, H. Yokoyama and O. Yamauchi, *Angew. Chem., Int. Ed.*, 1999, **38**, 2401–2403.
22 S. Itoh, H. Nakao, L. M. Berreau, T. Kondo, M. Komatsu and S. Fukuzumi, *J. Am. Chem. Soc.*, 1998, **120**, 2890–2899.
23 M. J. Baldwin, D. E. Root, J. E. Pate, K. Fujisawa, N. Kitajima and E. I. Solomon, *J. Am. Chem. Soc.*, 1992, **114**, 10421–10431.
24 M. J. Henson, V. Mahadevan, T. D. P. Stack and E. I. Solomon, *Inorg. Chem.*, 2001, **40**, 5068–5069.
25 P. L. Holland, C. J. Cramer, E. C. Wilkinson, S. Mahapatra, K. R. Rodgers, S. Itoh, M. Taki, S. Fukuzumi, L. J. Que and W. B. Tolman, *J. Am. Chem. Soc.*, 2000, **122**, 792–802.